Muon bundles from cosmic-ray multi-W phenomena

D. A. Morris* and R. Rosenfeld†
Department of Physics, University of California at Los Angeles, Los Angeles, California 90024-1547
(Received 20 May 1991)

The consequences of novel high-energy electroweak phenomena are studied in the context of cosmic-ray physics. The production of many electroweak gauge bosons ($\simeq 30-100$) by cosmic rays gives rise to large zenith-angle multimuon events which are free of background. We find detection rates of up to a few events per year for neutrino-induced phenomena in detectors currently under construction.

I. INTRODUCTION

Recently there has been much interest in the possibility that novel standard-model electroweak phenomena characterized by the production of $\simeq 30-100$ electroweak gauge bosons may exist above thresholds typically in the 4–20-TeV range [1]. The proposed processes may be manifestations of instanton-induced baryon-number plus lepton-number ($B+L$) violation [2] or consequences of the infrared structure of electroweak interactions [3,4]. In this paper we address the possibility of observing or constraining such phenomena in the realm of cosmic-ray physics which, until the construction of the appropriate terrestrial accelerators, provides the only window to the relevant energy range.

In the standard model, baryon number, lepton number, or combinations thereof are classical global symmetries of the Lagrangian and hence are not required to be anomaly-free: they may be violated at the quantum level. Because of the anomaly, a change in $B+L$ may be related to a transition between topologically inequivalent sectors of the electroweak vacuum which are separated by energy barriers of the order 10–15 TeV. Using a semiclassical approximation, 't Hooft [5] calculated the amplitude for tunneling between different sectors and obtained a disappointingly small result proportional to $e^{-8\pi^2/g^2}\approx 10^{-86}$, where $g=e/\sin\theta_W$ is the SU(2) coupling constant; the realization of $B+L$ violation in this manner appeared impractical.

At low energies (compared to the barrier energy) potentially amenable to experiment, $(B+L)$-violating processes are described by an effective pointlike interaction with a constant, albeit exponentially small coupling strength. Ringwald and Espinosa [2] noted that, due to enormous compensating phase-space factors, one may obtain rapidly rising cross sections for $(B+L)$-violating processes involving many, $\sim 30-100$, final-state gauge bosons and Higgs particles. Though there has been controversy [6,7] regarding the validity of the approximations used, the generic features of large cross-section $(B+L)$-violating processes consist of high-multiplicity final states above an energy threshold in the multi-TeV range with cross sections ≈ 1 pb, if such processes exist at all.

Aside from multi-W phenomena appearing in $B+L$ violation, there have also been suggestions that even in $(B+L)$-conserving processes, there may be large-cross-section, high-multiplicity phenomena associated with the breakdown of perturbation theory [3]. Some authors have interpreted these results as a consequence of the infrared structure of the electroweak theory [4]. At energies much larger than M_W, particles carrying SU(2) quantum numbers are surrounded by a cloud of virtual gauge bosons, in much the same way that quarks at high energies are surrounded by virtual gluons. The finite size of the gauge-boson cloud, of the order of $1/M_W$, would give rise to a geometrical (black-disk) cross section $\sigma\approx\pi/M_W^2$. Cross sections up to 10 μb and threshold energies from 4–20 TeV for the production of these multi-W events with average multiplicity $\langle n_W\rangle\simeq 4\pi/g^2\simeq 30$ have been discussed in the literature.

The prospects of observing multi-W processes at future accelerators have been investigated by other authors. Farrar and Meng [8], using a point cross section of the form $\hat{\sigma}=\theta(\sqrt{\hat{s}}-17\text{ TeV})16\pi/\hat{s}$, which saturates the unitarity limit, found a $(B+L)$-violation cross section of 1.5 pb at the Superconducting Super Collider (SSC), which is in principle observable. Ringwald, Schrempp, and Wetterich [9] have studied more general multi-W events with point cross sections parametrized by the threshold energy $\sqrt{\hat{s}_0}$ and a constant cross section $\hat{\sigma}_0$: $\hat{\sigma}=\hat{\sigma}_0\theta(\sqrt{\hat{s}}-\sqrt{\hat{s}_0})$. For $\hat{\sigma}_0=1$ nb, they conclude that these processes can be seen at the CERN Large Hadron Collider (LHC), SSC, and the European Long Intersecting Storage Accelerator (Eloisatron) for threshold energies less than 11, 28, and 130 TeV, respectively.

However, aside from future Earth-based accelerators, multi-W phenomena may also be initiated by very-high-energy cosmic rays. Multiple penetrating muons, also known as muon bundles or multimuon events, would arise from the decay of the many gauge bosons produced and could in principle be detected at underground experiments such as MACRO (Monopole, Astrophysics, Cosmic-Ray Observatory) [10] and DUMAND (Deep Underwater Muon and Neutrino Detector) [11]. As we discuss briefly in Sec. VII, one might also be able to exploit other features of multi-W phenomena such as the anomalous longitudinal or transverse development of air showers. In this paper we limit our attention to the ener-

getic multimuon characteristics of multi-W events and investigate how such phenomena may be identified in underground detectors.

Multi-W events may be initiated by either cosmic-ray protons interacting in the Earth's atmosphere or by cosmic-ray neutrinos interacting in the atmosphere or inside the Earth. However, because of large competing QCD cross sections, the signal for proton-initiated multi-W events is very small, as we will demonstrate in Sec. V. Therefore we concentrate on cosmic-ray neutrino-initiated multi-W events. Specifically, we will demonstrate that muon bundles at large zenith angles provide a signature free of background for neutrino-induced multi-W phenomena.

Nonstandard high-energy neutrino interactions have been suggested previously in the context of composite models [12] where colored subconstituents of neutrinos interact with typical QCD cross sections at energies larger than the compositeness scale. Since both neutrinos and photons come from pion decays, neutrinos produced in x-ray binary systems should be as abundant as high-energy photons and there has been speculation that nonstandard neutrino interactions could explain anomalous muon-rich signals from the direction of Cygnus X-3 [13].

This paper is organized as follows. In Sec. II we parametrize the point cross section for multi-W events and compare proton-proton and neutrino-nucleon cross sections of this new interaction with the usual QCD and electroweak cross sections. In Sec. III we discuss the general features of the underground detection of muons produced from neutrinos. In Sec. IV we outline the formalism used to compute underground multimuon event rates from multi-W phenomena and apply the results to proton- and neutrino-induced interactions in Secs. V and VI, respectively. We discuss our results and their limitations in Sec. VII and draw our conclusions in Sec. VIII.

II. PARAMETRIZATION OF MULTI-W PROCESSES

The generic hard subprocess we wish to consider is the inclusive production of n_W W bosons:

$$A+B\rightarrow n_W W+X\ , \tag{1}$$

where A and B are weakly interacting quarks or leptons. Since we will ultimately concentrate on the detection of muons arising from the decays of vector bosons, one might argue that we should be interested in the inclusive production of W *and* Z bosons. In response, we interpret the right-hand side of Eq. (1) heuristically and consider n_W to be the "effective" number of W bosons. For example, if the number of prompt muons from vector-boson decay is used as a benchmark, then two Z bosons [with branching ratio $B(Z\rightarrow\mu^+\mu^-)\approx 3\%$] are roughly equivalent to one W boson for which $B(W^+\rightarrow\mu^+\nu_\mu)\approx 11\%$. Moreover, since we are concerned with cases where the final state is overwhelmingly composed of vector bosons, we will approximate the final state as consisting *exclusively* of n_W W bosons. In this sense our subsequent parametrization of multi-W processes is intended to embody only the gross overall characteristics of the final state. While such a parametrization is well suited to our immediate goals, one is cautioned against associating our parametrization with the details of any particular dynamical model.

In the interest of simplicity we parametrize the threshold behavior of the hard subprocess cross section by a step function

$$\hat{\sigma}_{n_W}(\sqrt{\hat{s}})=\hat{\sigma}_0\theta(\sqrt{\hat{s}}-\sqrt{\hat{s}_0})\ , \tag{2}$$

where the threshold energy $\sqrt{\hat{s}_0}$ is in the range $4<\sqrt{\hat{s}_0}<20$ TeV and $\hat{\sigma}_0<10$ μb. In addition we assume the subprocess cross section to be independent of the nature of A and B, requiring only that they couple directly to W and Z bosons.

We next fold the hard cross section with structure functions relevant to processes of interest. Within our parametrization the proton-proton (pp) multi-W cross section is given by

$$\sigma^{pp}_{n_W}(\sqrt{s})=\sum_{ij}\frac{1}{1+\delta_{ij}}\int dx_1\,dx_2\,f_i(x_1)f_j(x_2)\times\hat{\sigma}_{n_W}(\sqrt{x_1x_2s})\ , \tag{3}$$

where s is the proton-proton invariant mass squared and $f_i(x_1)$ is the number density of partons of type i carrying a fraction x_1 of the total proton momentum. As in Refs. [4,8] we evaluate all structure functions at a fixed scale $Q^2=M_W^2$ characteristic of the weak scale of the processes. We assume that the discrete sum extends over all combinations of weakly interacting proton constituents, that is, everything except gluons. In specific scenarios such as the instanton-induced $(B+L)$-violating processes of Ref. [2] not all possible parton combinations are included in the discrete sum and it is in this sense that our parametrization does not reflect a specific model. In a similar manner the neutrino-nucleon (νN) cross section is given by

$$\sigma^{\nu N}_{n_W}(\sqrt{s})=\sum_i\int dx\,f_i(x)\hat{\sigma}_{n_W}(\sqrt{xs})\ , \tag{4}$$

where again $f_i(x)$ is the number density of parton species i in the proton evaluated at $Q^2=M_W^2$ and the sum over i does not include gluons.

In Fig. 1 we present the scaled functions for $\sigma^{pp}_{n_W}(\sqrt{s})$ and $\sigma^{\nu N}_{n_W}(\sqrt{s})$. Their applicability is determined by the structure functions employed. We use the Eichten-Hinchliffe-Lane-Quigg (EHLQ) structure functions [14] valid for $x>10^{-4}$ and extend them by the Gribov-Levin-Ryskin ansatz [15] as described in Refs. [16,17], which in principle extends the useful region to $x\geq 10^{-8}$. This translates to a region of applicability $\sqrt{s}/\sqrt{\hat{s}_0}<10^4$ in Fig. 1, which is more than adequate for our purposes.

A few preliminary remarks will put the cross sections of Fig. 1 in perspective and set the stage for our subsequent analysis. First consider the pp cross section in the context of cosmic-ray phenomena. In the energy region of interest ($4<\sqrt{s}<20$ TeV) the growing pp total cross section deduced from air-shower experiments and anticipated from QCD interactions is of the order of 100 mb

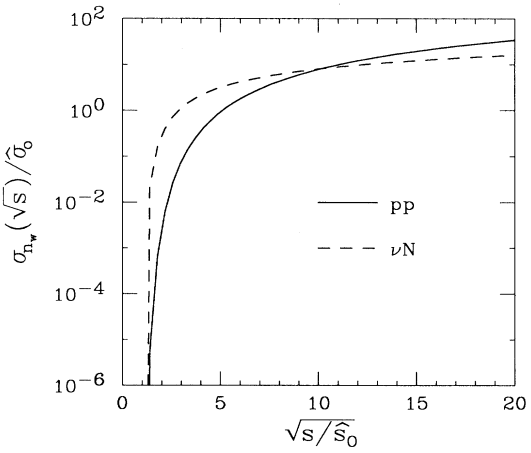

FIG. 1. The universal curves parametrizing the production of n_W W bosons in proton-proton (pp) and neutrino-nucleon (νN) interactions, where $\sqrt{s}$ is the total center-of-mass energy. The curves are scaled by the point cross section $\hat{\sigma}_0$ and the subprocess threshold energy $\sqrt{\hat{s}_0}$.

[18]. By comparison, if we liberally set $\hat{\sigma}_0 = 10$ μb and $\sqrt{\hat{s}_0} = 4$ TeV in $\sigma^{pp}_{n_W}(\sqrt{s})$, then $\sigma^{pp}_{n_W}(\sqrt{s})/\sigma^{pp}_{\rm QCD}(\sqrt{s}) \lesssim 10^{-3}$ where there is any appreciable proton flux. In Sec. V we discuss the implications of trying to pick out proton-induced multi-W events against a large QCD background.

Neutrino-induced multi-W events do not suffer the problem of large competing processes as is the case for protons. In the energy range of interest to us, conventional νN charged-current (CC) cross sections are in the range 1–10 nb [16,17]. Hence, above the multi-W threshold, $\sigma^{\nu N}_{\rm CC}(\sqrt{s})$ does not necessarily overwhelm $\sigma^{\nu N}_{n_W}(\sqrt{s})$. It is this possibility of small losses to competing processes that makes neutrino-induced multi-W phenomena an attractive channel to study.

III. NEUTRINO-INDUCED MULTI-W PHENOMENA

Let us restrict our attention to neutrino-induced multi-W phenomena. The fraction of cosmic neutrino flux interacting in the atmosphere is $1-\exp(-N_A \sigma^{\nu N}_{\rm tot} X_0)$ where N_A is Avogadro's number and X_0 (g/cm^2) is the amount of atmosphere traversed. [In order to maintain consistency with the notation of other authors we use $N_A = 6.02\times 10^{23}$ with the understanding that one associates units of g^{-1} with N_A. We adhere to the common practice of expressing lengths in units of g/cm^2. For materials of uniform density, physical distances are recovered by dividing lengths (in g/cm^2) by the density (~ 2.6 g/cm^3 for standard rock).] The largest cross sections we shall consider are of the order $\sigma^{\nu N}_{n_W}(\sqrt{s}) \sim 10$ μb which corresponds to 1–17 % of the interactions occurring in the atmosphere for $X_0 \sim 1000$–$30\,000$ g/cm^2 (for normal/oblique incident neutrino flux). Consequently, the majority of neutrino-induced multi-W events occur in the Earth. However, unless such events occur completely inside an underground detector, all produced particles except for neutrinos and muons are quickly absorbed by the surrounding rock and go undetected.

In the relevant energy range the anticipated cosmic neutrino flux is sufficiently small to rule out the possibility of observing completely contained multi-W events in a realistic amount of time in a reasonable size detector. As a consequence we must look for the muon and/or neutrino products of a multi-W event. We consider both these possibilities in turn.

We characterize an underground detector by its depth D and a threshold energy $E_{\rm min}$. The threshold energy $E_{\rm min}$ is roughly the minimum energy required of a muon as it enters the detector in order that it passes completely through the detector and leaves an unambiguous track. Subsequently, by detected muons we mean muons which reach the detector with energies greater than $E_{\rm min}$. Typical existing and proposed detectors have $D \simeq 100$–4000 m and $E_{\rm min} \simeq 1$–100 GeV.

An underground muon detector has a sensitive volume determined by the maximum distance muons can travel in rock before they lose all their energy. For example, a 100-TeV muon penetrates approximately 11 000 hg/cm^2 (~ 4 km) of rock (1 hg = 100 g) before its energy drops below 100 GeV. Hence a prerequisite for detecting a neutrino-induced multi-W event via muons is that the interaction occur within a few kilometers of the detector.

In practice underground muon detectors are also used as neutrino detectors. By extending a muon trajectory in an underground detector back into the surrounding rock and towards the surface of the Earth, one can calculate the minimum energy of a muon of atmospheric origin necessary to penetrate to the detector. Knowing the muon energy-range relation in rock, one quickly deduces that upward-going muons in underground detectors must originate from neutrino interactions in the surrounding rock. Such a strategy has repeatedly been applied to the detection of the flux of atmospheric neutrinos [19,20].

In principle it is possible to detect the neutrinos produced in a multi-W event. The advantage of detecting prompt neutrinos over prompt muons is that the original interaction does not have to occur within a few kilometers of the underground detector so that the potentially detectable signal rate increases. The penalty paid, of course, is the relatively small probability that a neutrino on a detector trajectory will actually undergo a charged-current interaction close to the detector and give rise to a detectable muon. In Secs. V and VI we demonstrate quantitatively that, as suspected, the geometrical advantage gained falls well short of compensating for the small neutrino detection efficiency.

IV. CALCULATION OF THE MULTIMUON SIGNAL RATE

In this section we discuss the calculation of the underground detection rate of multimuon signals from multi-W events. Calculations of this genre have been performed previously in the context of detecting downward-going

atmospheric muon bundles [21,22] and upward-going atmospheric neutrinos [23,24] so that elements of these well-known results will necessarily appear as a subset of our work. We will consider both proton- and neutrino-induced multi-W phenomena which occur in the atmosphere or inside the Earth, respectively. Interactions inside the Earth giving rise to potentially detectable bursts of muons and neutrinos suggest a unique signature in underground detectors for multi-W phenomena: large-zenith-angle muon bundles.

Rather than presenting a general derivation of our equations (which would require defining many intermediate quantities), we will instead simply state our results and then outline the implicit assumptions. Initially we will concentrate on the calculation of the detection of prompt multimuons from both proton- and neutrino-induced multi-W phenomena. At the end of this section we indicate how the formalism is modified if one considers the possibility of detecting the prompt neutrinos (produced in association with the prompt muons) from W decay.

We will take a probabilistic approach to the calculation of the multimuon signal rate by considering the fate of a single incident cosmic projectile (either a neutrino or proton) and later convoluting the result with the relevant cosmic flux. Consider a cosmic projectile of energy E initially separated from the detector by an amount X of rock. Under the conditions outlined below, the probability that this projectile gives rise to a multi-W event with k muons detected in coincidence is given by

$$P_{k\mu}(E,X)=\frac{n_\mu! N_A}{(n_\mu-k)!k!}\int_0^X dX' e^{-N_A\sigma_{\rm tot}(X-X')} \times\sigma_{n_W}\tilde{p}_\mu^{\,k}(1-\tilde{p}_\mu)^{n_\mu-k}, \quad (5)$$

where n_μ is the number of collimated muons produced in a multi-W event. The total interaction cross sections are given by

$$\sigma_{\rm tot}^{\nu N}=\sigma_{\rm CC}^{\nu N}+\sigma_{n_W}^{\nu N}, \qquad \sigma_{\rm tot}^{pp}=\sigma_{\rm QCD}^{pp}+\sigma_{n_W}^{pp} \quad (6)$$

for neutrino and proton projectiles, respectively, with the understanding that all cross sections are evaluated at $\sqrt{s}=\sqrt{2m_pE}$.

The quantity $\tilde{p}_\mu$ in Eq. (5), which may be interpreted as the detection probability of a single "typical" muon produced in a multi-W event, is defined as

$$\tilde{p}_\mu(E,E_{\rm min},X')=\int_{E_{\rm min}}^E dE_\mu \frac{1}{n_\mu}\frac{dn_\mu}{dE_\mu}p_\mu(E_\mu,E_{\rm min},X') . \quad (7)$$

We stipulate a "typical" muon because $\tilde{p}_\mu(E,E_{\rm min},X')$ is the result of weighting $p_\mu(E_\mu,E_{\rm min},X')$ (the probability that a muon of definite energy E_μ traverses an amount X' of rock with $E_\mu>E_{\rm min}$) by $(1/n_\mu)(dn_\mu/dE_\mu)$ (the laboratory energy distribution of the muons produced in a multi-W event). We will discuss forms for $(1/n_\mu)(dn_\mu/dE_\mu)$ and $p_\mu(E_\mu,E_{\rm min},X')$ later.

The conditions under which Eqs. (5)–(7) apply are as follows.

(1) We assume that, in the hard subprocess rest frame, the n_W W bosons are distributed isotropically and share the available energy $\sqrt{\hat{s}}$ equally.

(2) We assume that the cosmic projectile energy E is in the interval $E_0<E<n_wE_0$, where $E_0=\hat{s}_0/2m_p$ is the threshold above which multi-W phenomena occur. We thus exclude cascade phenomena in which secondary hadrons and leptons produced in the decays of the n_W W bosons are themselves able to initiate multi-W events leading to a geometric increase in the multiplicity. In practice, this intriguing scenario is suppressed for a variety of reasons. For secondary hadrons the largest multi-W cross sections we consider are always substantially smaller than the competing QCD cross sections, so it is always more likely that an energetic hadron undergoes a QCD interaction instead of initiating a multi-W event. Only muons and neutrinos, due to their small competing process cross sections, are likely candidates for perpetuating cascade phenomena. Furthermore, if the cosmic projectile energy spectrum falls off sharply, the majority of multi-W events occur just above E_0 and the restriction $E<n_WE_0$ is not an issue. In practice, we will apply Eq. (5) even for $E>n_WE_0$ and hence conservatively treat all multi-W phenomena as being of the non-cascade variety.

(3) We will assume $n_\mu=n_W/9$, corresponding to the retention of only prompt muons from $W^+\to\mu^+\nu_\mu$. Other possible sources of muons are the weak decays of mesons such as pions and kaons. However, if the multi-W event occurs underground (as will be relevant to neutrino projectiles) the produced pions and kaons undergo inelastic strong interactions in the surrounding rock before they have a chance to decay, and hence they do not contribute muons. Though not so obvious, a similar fate often awaits charmed mesons. Finally, muons from τ decay are possible but they can be neglected relative to the prompt muons.

The approximation $n_\mu=n_W/9$ is less straightforward for atmospheric interactions relevant to proton projectiles. In this case the multitude of pions, kaons, etc. produced in hadronic air showers will have the opportunity to decay and produce muons in addition to the prompt muons. For example, a typical atmospheric shower initiated by a 100-TeV proton interacting through usual strong-interaction channels contains hundreds of muons with energies above a few GeV [25]. On general grounds we expect a similar number of muons in atmospheric multi-W events. However, of these hundreds, the overwhelming majority do not have sufficient energy to penetrate to a deep underground detector. Even the most energetic nonprompt muons, due to the hadronization process, are generally less energetic than prompt muons. Consequently, the detection probability of nonprompt muons generally decreases more rapidly, as a function of zenith angle, than that of prompt muons. We make the pessimistic approximation $n_\mu=n_W/9$ for the case of proton projectiles by anticipating its application at zenith angles beyond which the background of multimuons from generic QCD events is negligible.

For the time being we assume that all n_μ muons are prefectly collimated along the direction of the motion of the incident cosmic projectile. In Sec. VI we examine the lateral spread of muons for observable processes.

Combining the above three assumptions, one deduces that the normalized laboratory energy distribution of the prompt muons from neutrino-initiated phenomena is given by the step function

$$\frac{1}{n_\mu}\frac{dn_\mu}{dE_\mu}=\frac{n_W}{E_\nu}\theta\left[\frac{E_\nu}{n_W}-E_\mu\right] . \tag{8}$$

The analogous muon energy distribution for proton-induced multi-W phenomena depends on the fraction of the proton momentum carried by the projectile quark involved in the hard subprocess. Rather than introducing this complication, it is sufficient to consider the most optimistic scenario in which the relevant quark always carries the full proton momentum so that Eq. (8) is still valid.

The muon detection probability $p_\mu(E_\mu,E_{\min},X')$ embodies the various mechanisms by which muons lose energy in rock. In our calculation we employ the approximate muon energy-range relation

$$-\frac{dE_\mu}{dX}=\alpha(E_\mu)+\beta(E_\mu)E_\mu , \tag{9}$$

where the coefficient $\alpha(E_\mu)$ accounts for ionization losses and $\beta(E_\mu)$ accounts for energy losses due to bremsstrahlung, pair production, and photonuclear interactions. For calculations we have used the parametrizations of $\alpha(E_\mu)$ and $\beta(E_\mu)$ from Ref. [26] and Ref. [27], respectively. By using Eq. (9) we are neglecting the stochastic effects of range straggling which may become important for muon energies above 10^5 GeV. Our simple approach may incur errors in the neighborhood of 30% when calculating the differential energy loss of very-high-energy muons [28]; such uncertainties at this stage will not affect our final conclusions. Within our approximation of a deterministic energy-range relationship we have the step function

$$p_\mu(E_\mu,E_{\min},X')=\theta(E_\mu-E'_\mu(E_{\min},X')) , \tag{10}$$

where E'_μ is the solution of

$$X'=\int_{E_{\min}}^{E'_\mu}\frac{dE}{\alpha(E)+\beta(E)E} . \tag{11}$$

For illustrative purposes we plot $E'_\mu(E_{\min},X')$ in Fig. 2 and $\tilde{p}_\mu(E,E_{\min},X')$ in Fig. 3 for a few representative neutrino energies. As can be noted from Fig. 3, $\tilde{p}_\mu(E,E_{\min},X')$ reflects the step function nature of Eq. (10) and implies that if a multi-W event occurs close ($\simeq$ few km) to the detector, the prompt muons are almost certainly observed in the detector.

The differential flux of detected events with k muons in coincidence originating from multi-W phenomena, $dN_{k\mu}/(dA\,dt\,d\Omega)$, may be obtained by convoluting $P_{k\mu}(E,X)$ of Eq. (5) with the cosmic projectile flux $j\equiv dN/(dA\,dt\,d\Omega\,dE)$ (which we discuss in Secs. V and VI) to yield

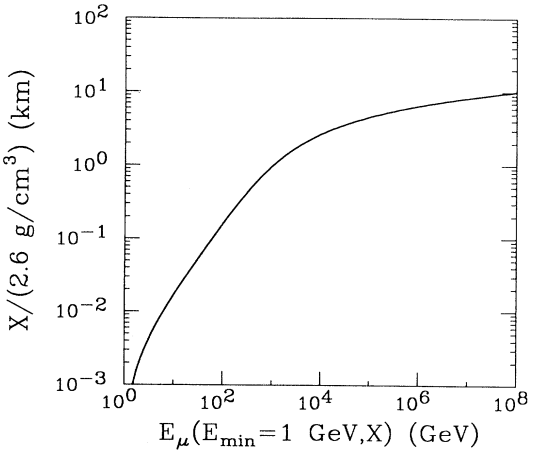

FIG. 2. The muon energy-range relation in standard rock ($Z=11$, $A=22$, $\rho=2.6$ g/cm^3).

$$\frac{dN_{k\mu}}{dA\,dt\,d\Omega}=\int_{E_{\min}}^{\infty}dE\,P_{k\mu}(E,X)j , \tag{12}$$

where

$$X=\rho[\sqrt{(R_\oplus-D)^2\cos^2\theta+2DR_\oplus-D^2}-(R_\oplus-D)\cos\theta] \tag{13}$$

is the distance from the detector (at a depth D) to the surface of the Earth (of radius $R_\oplus$) as a function of the zenith angle θ, and ρ is the rock density.

As promised we will briefly outline how the above formalism is modified for the detection of k prompt neutrinos in coincidence arising from neutrino- or proton-induced multi-W events. In particular, the expression for $P_{k\mu}(E,X)$ in Eq. (5) is still valid if one substitutes for $\tilde{p}_\mu$

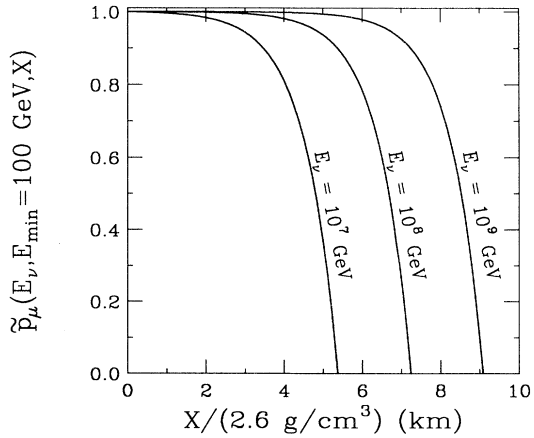

FIG. 3. Curves of $\tilde{p}_\mu(E_\nu,E_{\min}=100$ GeV, $X)$ for $n_W=30$ in standard rock. $\tilde{p}_\mu(E_\nu,E_{\min}=100$ GeV, $X)$ is the detection probability for a typical muon produced in an underground multi-W event at a distance X from the detector.

the analogous quantity

$$\tilde{p}_\nu(E,E_{\min},X')=\int_{E_{\min}}^{E} dE'_\nu \frac{n_W}{E}\theta\left[\frac{E}{n_W}-E'_\nu\right] \times p_\nu(E'_\nu,E_{\min},X') , \quad (14)$$

where

$$p_\nu(E'_\nu,E_{\min},X')=\int_0^{X'} dX'' \int_{E_{\min}}^{E'_\nu} dE'_\mu N_A e^{-N_A\sigma_{CC}^{\nu N}(X'-X'')} \times \frac{\partial\sigma_{CC}^{\nu N}}{\partial E'_\mu} p_\mu(E'_\mu,E_{\min},X'') . \quad (15)$$

The function $p_\nu(E'_\nu,E_{\min},X')$ is the probability that a neutrino of energy E'_ν at a distance X' undergoes a charged-current interaction and gives rise to a detected muon, a standard quantity in the underground detection of neutrinos [29]. Comparing $\tilde{p}_\mu(E_\nu,E_{\min},X)$ of Fig. 3 with $\tilde{p}_\nu(E_\nu,E_{\min},X)$, which we plot in Fig. 4, we note that the detection probability for neutrinos is orders of magnitude smaller than the corresponding probability for muons due to the additional charged-current interaction required.

V. PROTON-INDUCED MULTI-W PHENOMENA

As a demonstration of the framework outlined in Sec. IV we consider the case of proton-initiated multi-W phenomena. In the process of this exercise we wish to show why proton-initiated phenomena are not well suited to the detection of underground muons. On the constructive side, we will have the opportunity to discuss the dominant source of multimuon background and we will carry that knowledge to Sec. VI where we discuss the more promising neutrino-induced multi-W phenomena.

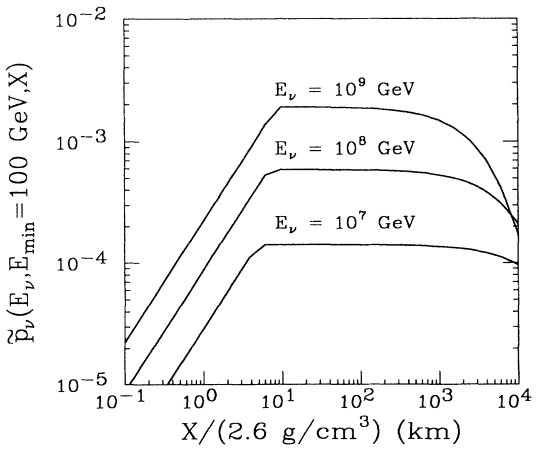

FIG. 4. Curves of $\tilde{p}_\nu(E_\nu,E_{\min}=100\ \text{GeV}, X)$ for $n_W=30$ in standard rock. $\tilde{p}_\nu(E_\nu,E_{\min}=100\ \text{GeV}, X)$ is the detection probability of a typical neutrino produced in an underground multi-W event at a distance X from the detector.

The detection rate of k muons in coincidence from proton-induced multi-W phenomena is given by

$$\frac{dN_{k\mu}^p}{dA\,dt\,d\Omega}=\int_{E_{\min}}^{\infty} dE_p\, P_{k\mu}^p(E_p,X) j_p , \quad (16)$$

where j_p is the differential cosmic-ray proton flux and $P_{k\mu}^p$ is the probability of Eq. (5) specific to a proton projectile:

$$P_{k\mu}^p(E_p,X)=\frac{n_\mu! N_A}{(n_\mu-k)!k!}\int_0^X dX' e^{-N_A\sigma_{\text{tot}}^{pp}(X-X')} \times\sigma_{n_W}^{pp}\tilde{p}_\mu^k(1-\tilde{p}_\mu)^{n_\mu-k} . \quad (17)$$

Since $\sigma_{\text{tot}}^{pp}\simeq\sigma_{\text{QCD}}^{pp}\simeq 100$ mb, the proton interaction length $X_{\text{int}}=1/(\sigma_{\text{QCD}}^{pp}N_A)\simeq 20$ g/cm^2 is much smaller than the atmospheric depth $X_{\text{atm}}\simeq 1000$ g/cm^2; thus most events occur high in the atmosphere before the proton flux is attenuated by QCD interactions. The small proton interaction length allows us to approximate

$$P_{k\mu}^p(E_p,X)=\frac{n_\mu!}{(n_\mu-k)!k!}\frac{\sigma_{n_W}^{pp}}{\sigma_{\text{tot}}^{pp}}\tilde{p}_\mu^k(1-\tilde{p}_\mu)^{n_\mu-k} , \quad (18)$$

where $\tilde{p}_\mu(E_p,E_{\min},X)$ is evaluated at X given by Eq. (13). The ratio $\sigma_{n_W}^{pp}/\sigma_{\text{tot}}^{pp}$ already indicates that the proton-initiated multi-W signal is on the order of 1000 times smaller than the usual QCD processes. Furthermore, since both types of processes are initiated in the atmosphere, the underground distribution of muons will be very similar.

The dominant background for multi-W events comes from muons created by the decay of pions and kaons produced in the atmosphere by high-energy cosmic rays via ordinary QCD interactions. In order to estimate the signal and background, we use the constant mass composition model of Refs. [22,30] for the cosmic proton spectrum:

$$j_p=\begin{cases} 1.72\left[\dfrac{1\ \text{GeV}}{E}\right]^{2.71}\ \text{cm}^{-2}\,\text{sec}^{-1}\,\text{sr}^{-1}\,\text{GeV}^{-1} , \\ E\le 2\times10^6\ \text{GeV} , \\ j_p(E=2\times10^6\ \text{GeV})\left[\dfrac{2\times10^6\ \text{GeV}}{E}\right]^3 , \\ E>2\times10^6\ \text{GeV} . \end{cases} \quad (19)$$

We obtain a pessimistic estimate of the background multimuon rate by assuming that cosmic-ray protons impart all of their energy to three muons and three neutrinos (assuming that this is the background relevant to a signal consisting of $n_W/9\simeq 3$ muons). Using j_p of Eq. (19) and the muon energy-range relation of Eq. (10) we see in Fig. 5 that the detection rate of background muon bundles decreases precipitously above zenith angles of approximately 84° for $E_{\min}=100$ GeV and a detector depth of 1.4 km of rock (approximately the depth of MACRO).

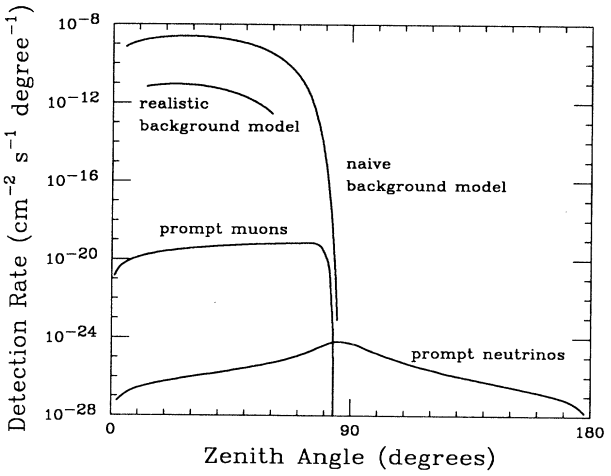

FIG. 5. The detection rate of multimuons produced in proton-induced multi-W events and the corresponding background. The curves assume a detector depth of 1.4 km in standard rock, $E_{\min}=100$ GeV, a multi-W threshold of $\sqrt{\hat{s}_0}=4$ TeV, and a point cross section $\hat{\sigma}_0=10$ μb with $n_W=30$. A detected event corresponds to two or more muons arriving at the detector simultaneously.

This falloff reflects the simple fact that all proton interactions occur in the atmosphere so that any produced muons must travel through at least 1.4 km of rock to reach the detector. The increase in the amount of rock with zenith angle and the logarithmic behavior of the muon energy-range relation results in the sharp falloff.

We can gauge the pessimism of our background normalization by comparing it with the more plausible estimate of the background rate for three or more muons using the model of Ref. [22], which parametrizes the various muon production and propagation processes in detail (albeit only for zenith angles less than 60°). We anticipate that, due to the softening effects of hadronization, muons from the decays of pions and kaons produced in competing generic QCD interactions will be less energetic than the prompt muons introduced in multi-W processes. Since muons from all sources must traverse the same amount of rock, the naive hope is that the energetic prompt multimuon signal may persist to large zenith angles. Unfortunately we cannot confirm this assertion quantitatively because there are no available parametrizations of the background multimuon rate for large zenith angles (i.e., $>60°$).

In Fig. 5 we also show the proton-initiated multi-W signal rate as a function of zenith angle. For purposes of illustration we characterize the multi-W phenomena by the production of $n_W=30$ W bosons above a threshold of $\sqrt{\hat{s}_0}=4$ TeV with a point cross section of $\hat{\sigma}_0=10$ μb. We define a signal event as the simultaneous arrival of two or more muons in the detector.

In Fig. 5 we show signal rates for the detection of both prompt muons and prompt neutrinos. The prompt muon signal decreases dramatically at large zenith angles for precisely the same reasons that the background decreases (as described above). The large competing QCD cross section forces the overall detection rate of prompt multimuons to be much smaller than the background. Moreover, the prompt multimuon signal is buried under our pessimistic background for all zenith angles. A realistic multimuon background calculation, in the spirit of Ref. [22], for zenith angles greater than 60° is clearly desirable. Even then, the absolute detection rate of proton-induced multi-W prompt muons may be negligible: the total rate for prompt muons in Fig. 5 (i.e., frivolously ignoring the overwhelming background and integrating over all zenith angles) is $\simeq 3\times 10^{-18}$ cm^{-2} sec^{-1}, less than one event in a thousand years in a MACRO-size detector. The proton-induced multimuon signal is clearly not feasible.

For completeness we also include in Fig. 5 the even smaller detection rate of prompt multineutrinos. In contrast with the prompt multimuon case, the curve corresponding to the detection of prompt neutrinos extends over all zenith angles, reflecting the relative transparency of the Earth to neutrinos. Though the background-free detection rate is negligible in this case, the persistence of the neutrino signal to large zenith angles foreshadows the more promising scenario of neutrino-induced multi-W events which we study in Sec. VI.

VI. NEUTRINO-INDUCED MULTI-W PHENOMENA

Hoping to elude the background of downward-moving muon bundles, we next consider neutrino-induced multi-W phenomena. In order to be quantitative, we must confront the issue of what to use for the high-energy cosmic neutrino flux j_ν. Little is known experimentally about the cosmic neutrino flux above 10^6 GeV, whereas we are interested in the flux above 8×10^6 GeV (corresponding to a threshold of 4 TeV for multi-W phenomena). The best constraints come from the Fly's Eye, an air-shower array sensitive to nitrogen scintillation light generated by extensive air showers with energies greater than 10^8 GeV [31]. We will organize our discussion by first discussing the constraints imposed by the Fly's Eye results and then by considering scenarios for j_ν in the intermediate range $8\times 10^6 < E_\nu < 10^8$ GeV. We then use the neutrino flux models to estimate the multimuon signal rates from neutrino-induced multi-W phenomena.

The Fly's Eye puts upper limits on the product of the flux times cross section for weakly interacting particles above 10^8 GeV; we will assume all such particles are neutrinos. If limits on the flux times cross section are interpreted as limits on the quantity [17]

$$I(E)=\int_E^\infty dE_\nu\, j_\nu \sigma_{\rm tot}^{\nu N}(E_\nu)\ , \qquad (20)$$

then the Fly's Eye results may be expressed as $I(10^8\ \text{GeV})<10^{-45}$, $I(10^9\ \text{GeV})<3.8\times 10^{-46}$, $I(10^{10}\ \text{GeV})<10^{-46}$, and $I(10^{11}\ \text{GeV})<3.8\times 10^{-47}$ (in units of sec^{-1} sr^{-1}). The limits are deduced from the nonobservation of downward-moving air showers within the Fly's Eye fiducial volume such that the shower axis is inclined 80 to 90° from the zenith at the point of impact on the Earth [31]. Geometry dictates that a shower meeting these criteria could only have been initiated by a particle

which had penetrated more than 3000 g/cm^2 of atmosphere before interacting, which excludes showers initiated by high-energy photons and hadrons (which have interaction lengths of approximately 45 g/cm^2). Since the Fly's Eye analysis assumes that the flux under investigation suffers no atmospheric attenuation before reaching the fiducial volume, the Fly's Eye limits apply to processes with cross sections less than 10 μb.

Strictly speaking, the integrand in Eq. (20) should contain an atmospheric attenuation factor of the approximate form $e^{-N_A \sigma_{\rm tot}^{\nu N} X_0}$, where $X_0 \simeq 3000-30\,000$ g/cm^2 characterizes the atmospheric depth of the Fly's Eye fiducial volume. While it would be an excellent approximation to neglect atmospheric attenuation if we were considering only usual charged-current neutrino interactions, we will at times contemplate multi-W point cross sections $\hat{\sigma}_0 \approx 10$ μb (implying even larger $\sigma_{n_W}^{\nu N}$) where it is not obvious, *a priori,* that we can neglect attenuation effects. Nevertheless, for reasons which will become apparent later, we may still neglect atmospheric attenuation for all ranges of the parameters we consider.

The logarithm of the Fly's Eye limits on $I(E)$ is well approximated by a linear function of the logarithm of the neutrino energy. Performing the corresponding linear least-squares fit and substituting the result in Eq. (20) leads to the constraint on the cosmic neutrino flux

$$j_\nu \le \frac{3.74\times10^{-42}\ \text{cm}^2}{\sigma_{\rm tot}^{\nu N}(E_\nu)} \times \left[\frac{1\ \text{GeV}}{E_\nu}\right]^{1.48} \text{cm}^{-2}\,\text{sec}^{-1}\,\text{sr}^{-1}\,\text{GeV}^{-1}\ , \quad (21)$$

which is valid for $10^8 \le E_\nu \le 10^{11}$ GeV. An inequality similar to Eq. (21) appears in Ref. [32] with an unoptimized fit of the Fly's Eye limits and $\sigma_{\rm tot}^{\nu N} = \sigma_{\rm CC}^{\nu N}$.

Since the cosmic neutrino flux for $8\times10^6 < E_\nu < 10^8$ GeV is relatively unconstrained by experiment, we are free to consider various options in that energy range. Though it would be conservative to assume a flat neutrino energy spectrum below 10^8 GeV, there is motivation to believe that the neutrino flux increases with decreasing energy. In the energy window below 10^8 GeV, which interest us, the atmospheric neutrino flux (e.g., from the decays of pions and kaons produced in generic atmospheric cosmic-ray interactions) is anticipated to be negligible [33]. However, there has been speculation that additional components of the neutrino flux may become relevant at energies round 10^8 GeV, whereby neutrinos may be produced, for example, by cosmic-ray processes in interstellar gas in our Galaxy [34], by accelerated protons interacting in the medium surrounding pulsars [35], or by other mechanisms in active galactic nuclei [36]. In deference to such speculations, but without committing ourselves to a specific mechanism, we will, in addition to assuming a flat spectrum below 10^8 GeV, also consider the possibility that the neutrino flux exhibits a power-law behavior $\sim 1/E_\nu^2$ below 10^8 GeV. Though the choice of a quadratic behavior is essentially arbitrary, we should keep in mind that we are only assuming this power-law behavior over the limited range $8\times10^6 < E_\nu < 10^8$ GeV. For consistency we will later check that a power-law behavior does not contradict the nominal experimental limits on the neutrino flux in this energy range.

In summary, we will use for the neutrino flux in Eq. (12), a spectrum which is flat below the Fly's Eye threshold,

$$j_\nu = \begin{cases} \dfrac{3.74\times10^{-42}\ \text{cm}^2}{\sigma_{\rm tot}^{\nu N}(E)} \left[\dfrac{1\ \text{GeV}}{E}\right]^{1.48}, & E \ge 10^8\ \text{GeV}\ , \\ j_\nu(E = 10^8\ \text{GeV})\ , & E < 10^8\ \text{GeV}\ , \end{cases} \quad (22)$$

$$j_\nu = \begin{cases} \dfrac{3.74\times10^{-42}\ \text{cm}^2}{\sigma_{\rm tot}^{\nu N}(E)} \left[\dfrac{1\ \text{GeV}}{E}\right]^{1.48}, & E \ge 10^8\ \text{GeV}\ , \\ j_\nu(E = 10^8\ \text{GeV}) \left[\dfrac{10^8\ \text{GeV}}{E}\right]^2, & E < 10^8\ \text{GeV}\ , \end{cases} \quad (23)$$

where j_ν is in units of cm^{-2} sec^{-1} sr^{-1} GeV^{-1}. For our calculation of $\sigma_{\rm tot}^{\nu N}$ we use the charged-current neutrino-nucleon cross section $\sigma_{\rm CC}^{\nu N}$ described in Ref. [16] and the multi-W cross section $\sigma_{n_W}^{\nu N}$ of Eq. (4).

In Fig. 6 we present the angular distribution of detected multi-W phenomena corresponding to the simultaneous arrival of two or more muons in a detector 1.4 km under the Earth. We show the individual contributions from the detection of multimuons and multineutrinos. The multimuon detection rate persists well beyond zenith angles of 84° where there is no background. A similar situation exists for the detection of multineutrinos but is of little practical value since the rate is always much smaller

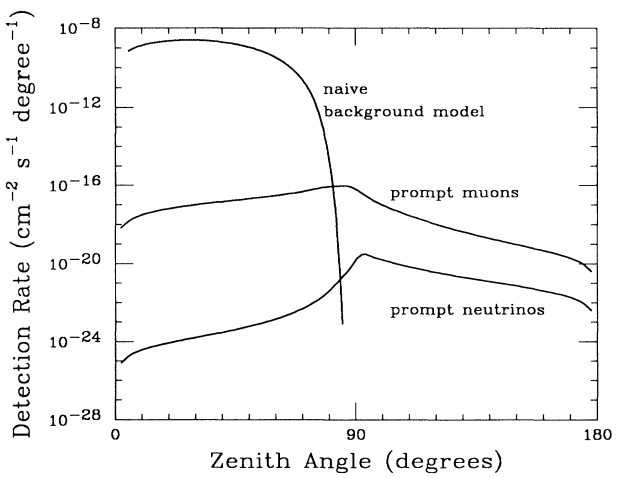

FIG. 6. The detection rate of multimuons produced in neutrino-induced multi-W events and the corresponding background. The curves assume a detector depth of 1.4 km in standard rock, $E_{\rm min} = 100$ GeV, a multi-W threshold of $\sqrt{\hat{s}_0} = 4$ TeV, and a point cross section $\hat{\sigma}_0 = 1$ nb with $n_W = 30$. A detected event corresponds to two or more muons arriving at the detector simultaneously.

TABLE I. Signal rate of multi-W events for which $n_W=30$. The signal corresponds to two or more muons in coincidence in a detector 4 km below the ocean surface ($\simeq$ DUMAND) with a threshold $E_{\min}=100$ GeV such that the zenith angle of the muon bundle is greater than 84°. Rates are in $\text{cm}^{-2}\,\text{sec}^{-1}$).

ν spectrum assumptions for $E_\nu > 10^8$ GeV	ν spectrum behavior for $E_\nu < 10^8$ GeV	$\sqrt{\hat{s}_0}$ (TeV)	$\hat{\sigma}_0=1$ nb	$\hat{\sigma}_0=100$ nb	$\hat{\sigma}_0=10$ μb
None	Flat	20	1.2×10^{-16}	4.0×10^{-16}	1.5×10^{-16}
None	Flat	4	1.3×10^{-15}	3.4×10^{-16}	2.5×10^{-19}
None	$\sim 1/E_\nu^2$	4	1.7×10^{-15}	6.6×10^{-16}	7.2×10^{-18}
$p+\gamma\to\nu X$	Flat	20	2.8×10^{-17}	1.6×10^{-16}	1.6×10^{-18}
$p+\gamma\to\nu X$	Flat	4	2.0×10^{-16}	2.4×10^{-17}	1.4×10^{-21}
$p+\gamma\to\nu X$	$\sim 1/E_\nu^2$	4	2.1×10^{-16}	2.6×10^{-17}	4.2×10^{-20}

than the multimuon rate.

In Tables I and II we collect the multimuon detection rates (for zenith angles greater than 84°) for neutrino-initiated multi-W phenomena for various cross sections, thresholds, and flux models corresponding roughly to the DUMAND and MACRO detectors, respectively. The cutoff of 84° is somewhat arbitrary but is chosen to ensure that the signal rate, when observable, is always orders of magnitude larger than our pessimistic background estimate; it is largely fortuitous that 84° is used in both Tables I and II since the respective detectors are at different depths and surrounded by different material.

Keeping in mind that one event per year in a detector with area 10^4 m^2 (approximately the size of DUMAND) corresponds to a detection rate of $\sim 3\times10^{-16}$ $\text{cm}^{-2}\,\text{sec}^{-1}$, we see that under optimal conditions multi-W phenomenon may indeed be observable. However, before drawing optimistic conclusions, let us reexamine the dependence on the neutrino flux.

The first two rows of Table I correspond to the neutrino flux of Eq. (22) which saturates the Fly's Eye limits above 10^8 GeV and assumes a flat spectrum below 10^8 GeV. The signal rates are marginal and correspond to 1–4 events per year in a 10^4-m^2 detector. For thresholds $\sqrt{\hat{s}_0}$ larger than ~ 14 TeV (corresponding to $E_\nu > 10^8$ GeV) these detection rates are optimized: they saturate the Fly's Eye constraints and are independent of the neutrino flux below 10^8 GeV.

The signal rate scenario brightens somewhat depending on how generously we exploit our lack of knowledge of the neutrino flux below 10^8 GeV. Increasing the flux below 10^8 GeV can potentially increase the signal rate if the multi-W threshold is below 14 TeV as demonstrated in the third row of Table I.

The dependence of the signal rates on the point cross section $\hat{\sigma}_0$, the threshold $\sqrt{\hat{s}_0}$, and the flux models may be appreciated by considering the special case of $\hat{\sigma}_0=10$ μb and $\sqrt{\hat{s}_0}=4$ TeV (even though this set of parameters does not lead to promising rates). Our requirement that muon bundles originate from large zenith angles implies that detected events correspond to relatively small values of $\sigma_{\text{tot}}^{\nu N}$ ($\lesssim 10$–100 nb). Hence, detectable events must occur close to threshold if $\hat{\sigma}_0$ is large. If in addition the cosmic neutrino energy at threshold is much below 10^8 GeV (as is true for the case under consideration), then the detectable signal rate originates from a portion of the neutrino spectrum which is unconstrained by the Fly's Eye limits; this explains the sensitivity of the detection rate to the form of the flux models below 10^8 GeV.

The special case $\hat{\sigma}_0=10$ μb, $\sqrt{\hat{s}_0}=4$ TeV also demon-

TABLE II. Signal rate of multi-W events for which $n_W=30$. The signal corresponds to two or more muons in coincidence in a detector 1.4 km ($\simeq$ MACRO) below the Earth with a threshold $E_{\min}=2$ GeV such that the zenith angle of the muon bundle is greater than 84°. Rates are in $\text{cm}^{-2}\,\text{sec}^{-1}$.

ν spectrum assumptions for $E_\nu > 10^8$ GeV	ν spectrum behavior for $E_\nu < 10^8$ GeV	$\sqrt{\hat{s}_0}$ (TeV)	$\hat{\sigma}_0=1$ nb	$\hat{\sigma}_0=100$ nb	$\hat{\sigma}_0=10$ μb
None	Flat	20	6.8×10^{-17}	2.6×10^{-16}	9.6×10^{-17}
None	Flat	4	6.9×10^{-16}	2.7×10^{-16}	2.1×10^{-19}
None	$\sim 1/E_\nu^2$	4	9.0×10^{-16}	4.8×10^{-16}	5.9×10^{-18}
$p+\gamma\to\nu X$	Flat	20	1.5×10^{-17}	1.1×10^{-16}	1.2×10^{-18}
$p+\gamma\to\nu X$	Flat	4	1.2×10^{-16}	2.0×10^{-17}	1.2×10^{-21}
$p+\gamma\to\nu X$	$\sim 1/E_\nu^2$	4	1.2×10^{-16}	2.1×10^{-17}	3.5×10^{-20}

strates why we are justified in neglecting atmospheric attenuation when extracting flux constraints from the Fly's Eye results: observable events necessarily correspond to $\sigma_{\rm tot}^{\nu N} \lesssim 10\ \mu$b for which there is little attenuation. The normalization of our low-energy flux extrapolations [Eqs. (22) and (23)] depend on $\sigma_{\rm tot}^{\nu N}(10^8\ {\rm GeV})$, where we demand consistency with the Fly's Eye results [Eq. (21)]. In this worst case, $\sigma_{\rm tot}^{\nu N}(10^8\ {\rm GeV}) \approx 15\ \mu$b corresponds to an underestimate of the flux normalization by no more than 25%, which we neglect.

We also consider the event rates expected if, instead of saturating the Fly's Eye limits above 10^8 GeV, we require the neutrino spectrum above 10^8 GeV to assume some theoretically motivated form. The dominant contribution to the flux of high-energy neutrinos ($E_\nu > 10^8$ GeV) is expected to arise from the decay of pions produced by the interaction $p+\gamma \rightarrow \pi N$ in which cosmic-ray protons ($E_p > 10^{11}$ GeV) scatter off the 2.7-K background radiation [37]. Using the appropriate transport equations, one may calculate the subsequent neutrino energy spectrum as a function of the shape, strength, and redshift of the proton source [38]. We will adopt a generic form for the ultra-high-energy neutrino spectrum which embodies the general features of the neutrino spectra of Ref. [38]. Namely, we will consider a model of the photoproduced neutrino flux in which the energy spectrum is flat below 10^9 GeV and falls as $\sim 1/E_\nu^{3.5}$ above 10^9 GeV:

$$j_\nu = \begin{cases} K\ , & E < 10^9\ {\rm GeV}\ , \\ K\left[\dfrac{10^9\ {\rm GeV}}{E}\right]^{3.5}\ , & E \geq 10^9\ {\rm GeV}\ , \end{cases} \tag{24}$$

where K is an overall normalization factor which we determine by demanding consistency with the Fly's Eye results above 10^8 GeV. Figure 7 plots the maximum values of K consistent with the Fly's Eye limits of Eq. (21).

Finally, we also consider a photoproduced neutrino spectrum where, below the Fly's Eye thresold, we include an additional component governed by a power law

$$j_\nu = \begin{cases} K\left[\dfrac{10^8\ {\rm GeV}}{E}\right]^2\ , & E < 10^8\ {\rm GeV}\ , \\ K\ , & 10^8\ {\rm GeV} \leq E < 10^9\ {\rm GeV}\ , \\ K\left[\dfrac{10^9\ {\rm GeV}}{E}\right]^{3.5}\ , & 10^9\ {\rm GeV} \leq E\ . \end{cases} \tag{25}$$

The signal rates corresponding to neutrino fluxes of Eqs. (24) and (25) are given in the last three rows of Table I. As anticipated, the rates are always smaller than the rates corresponding to the fluxes of Eqs. (22) and (23) which saturate the Fly's Eye constraints.

Not only are bundles of prompt muons the most promising signal but they are also an efficient signature. For the rates of Tables I and II approximately 90% of the detected bundles contain all $n_W/9 \approx 3$ prompt muons for $n_W = 30$. This feature contrasts with the situation for the feeble multineutrino signal which, due the small neutrino detection probability, consists almost exclusively of only two muons, even for large n_W.

In Fig. 8 we show the radial spread of muons within a muon bundle for $\sqrt{\hat{s}_0} = 4$ TeV and $\hat{\sigma}_0 = 1$ nb for bundles at zenith angles greater than 84°. The distributions include the effects of a variable momentum fraction carried by the struck quark, the assumed isotropic distribution of muons in the neutrino-quark frame, and multiple Coulomb scattering in the medium surrounding the detector. The distributions measure the deviation of a detected muon from the direction of the cosmic neutrino which initiated the multi-W interaction. The mean radial spread is 30 cm for a detector under 1.4 km of rock and 90 cm for a detector under 4 km of water. The larger radial spread for bundles observed in an underwater detector is largely a consequence of a larger effective detector size due to the lower density of water. Though included in the distributions, the effects of multiple Coulomb

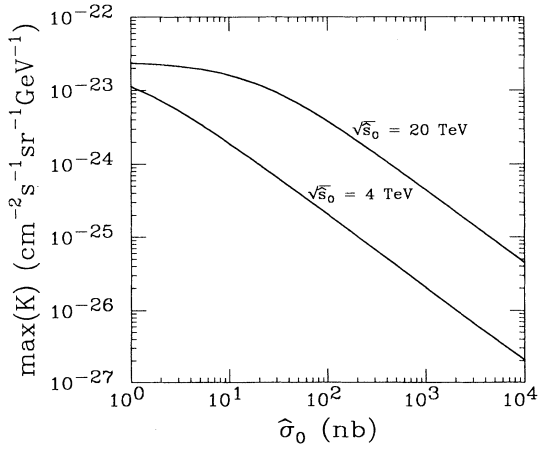

FIG. 7. The maximum normalization factor K consistent with the Fly's Eye limits and the generic photoproduced neutrino flux spectra of Eqs. (24) and (25).

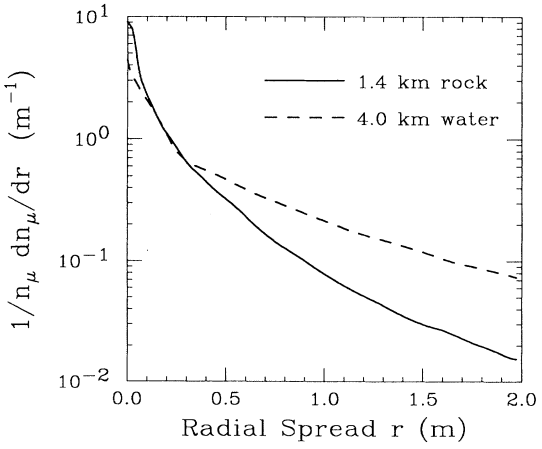

FIG. 8. Radial spread of muons in bundles at zenith angles greater than 84° for $\sqrt{\hat{s}_0} = 4$ TeV and $\hat{\sigma}_0 = 1$ nb.

scattering are generally negligible due to the large muon energies involved. Qualitatively similar distributions are obtained for other parameters.

VII. DISCUSSION

Though small, the signal rate of near-horizontal multimuon events lies tantalizingly close to the observation window of future detectors. Not surprisingly, the factors which limit us are the relatively small neutrino fluxes and the finite size of realistic detectors.

Of the various detection mechanisms considered, only neutrino-induced phenomena detected via prompt multimuons is feasible. As expected, the detection rate of multineutrino events is always negligible. We have also shown how the proton-induced multimuon signal is small and buried under the background which has a similar zenith-angle dependence.

The detection rates in Tables I and II correspond to $\lesssim 0.1$ events a year at MACRO (assuming an effective area of 500 m^2 seen by horizontal muons) and $\lesssim 5$ events a year at DUMAND (assuming an effective area of 10^4 m^2). These rates have understandable dependences on the parameters $E_{\min}$ and n_W. For example, varying $E_{\min}$ from 2 to 100 GeV in Table II decreases the detection rates by a few percent: this insensitivity is a result of muons from multi-W events having energies typically greater than hundreds of TeV when produced. Increasing n_W from 30 to 100 for $\sqrt{\hat{s}_0}=10$ TeV, $\hat{\sigma}_0=1$ nb, under conditions analogous to those of Table I, decreases the detection rate of 4.2×10^{-16} $cm^{-2}sec^{-1}$ by about 10%, a marginal decrease since the final-state energy must be shared among more particles. However, regardless of such insensitivities, the rates in Tables I and II should not be viewed as predictions but rather should be interpreted only as plausible order-of-magnitude estimates due to the uncertainties inherent in the assumptions we make.

The uncertainty in the cosmic neutrino flux is clearly the most critical factor affecting our results. Since our most promising detection rates are a consequence of saturating the Fly's Eye constraints, one may ask how close theoretically motivated flux models come to satisfying these requirements. Indeed, though the photoproduced neutrino flux expected from protons scattering off 2.7-K cosmic photons is typically an order of magnitude smaller than the Fly's Eye limits [39] (assuming only conventional charged-current neutrino interactions), our largest signal rates originate from neutrino energies on the order of 10^8 GeV. At these energies additional, yet speculative, contributions to the neutrino flux (such as from active galactic nuclei in Ref. [36]) are anticipated which can come close to saturating the Fly's Eye limits. Where relevant, the neutrino fluxes we imply are not significantly different from those motivated theoretically; whether the theoretical models are themselves justified is a separate issue.

As for the flux spectra that we extrapolate below 10^8 GeV, we have verified that we have not violated naive limits on the flux of high-energy neutrinos which come from the measured rate of single upward-going muons in underground detectors [19,20]. To do this, we considered the largest neutrino flux implied by Eq. (23) (corresponding to $\sqrt{\hat{s}_0}=4$ TeV, $\hat{\sigma}_0=1$ nb) and, using the resulting spectrum above $\hat{s}_0/2m_p\approx 8.5\times10^6$ GeV, we calculated the contribution to the flux of single, upward-going muons in a detector similar to Kamiokande [20] (depth ≈ 1 km, $E_{\min}=1.7$ GeV). Whereas Kamiokande measures a total flux of upward-going muons of $(2.05\pm0.18)\times10^{-13}$ $cm^{-2}sec^{-1}sr^{-1}$ (which is consistent with the rate expected from models of the atmospheric neutrino flux), we found a maximum additional contribution from neutrino energies above 8.5×10^6 GeV of $\simeq 0.06\times10^{-13}$ cm^{-2} $sec^{-1}sr^{-1}$, which is safely within the experimental uncertainties.

Below 10^8 GeV the neutrino fluxes of Eqs. (22)–(25) may be thought of as plausible extrapolations of the spectra extracted from the Fly's Eye limits. However, because of the relative lack of experimental constraints for $8\times10^6<E<10^8$ GeV, one may ponder the consequences of using a particular theoretical model. For example, consider the model of the cosmic neutrino flux from active galactic nuclei as suggested in Ref. [36], which gives a flux comparable to or larger than our naive extrapolations of Eqs. (22)–(25). By inserting the flux of Ref. [36] in the Fly's Eye constraint of Eq. (20) we obtain a corresponding constraint on the permitted ranges of $\sqrt{\hat{s}_0}$ and $\hat{\sigma}_0$. Specifically, we find that $\hat{\sigma}_0\lesssim 5$ nb for $\sqrt{\hat{s}_0}=4$ TeV and $\hat{\sigma}_0\lesssim 340$ nb for $\sqrt{\hat{s}_0}=20$ TeV which, under the conditions relevant to Table I with a DUMAND type detector, correspond to maximum detection rates of 4.2×10^{-15} and 1.4×10^{-16} $cm^{-2}sec^{-1}$, respectively.

Since we have not taken detector efficiencies into account, the specific characteristic of individual detectors may also be important. Though the detection rates we calculate are free of background, detectors such as MACRO and DUMAND are not optimized for the detection of near-horizontal muons: this may pose a problem for the multimuon signature we propose. Because of the relatively small detection rates, it is also clearly desirable to use the largest detector possible. However, the detector size may not be a realistic concern since planned terrestrial accelerators will most likely be operational before underground detectors larger than DUMAND exist. Nevertheless, the event rates we propose would provide an ample signal in future high-energy neutrino telescopes with areas on the order of 1 km^2, which may be required for other reasons, as advocated in Ref. [40]. Since the maximum multimuon signal rates we propose, $\sim10^{-15}$ $cm^{-2}sec^{-1}$, are the same as the single upward muon rate anticipated from point sources such as Cygnus X-3 [41], the technical complications associated with the detection of such rates should be similar.

We have examined only those cross sections and thresholds motivated by recent suggestions of novel phenomena in the standard model of electroweak interactions. If the cross sections are much larger than 10 μb we lose the desirable properties of neutrino-induced phenomena and our analysis using underground detectors suffers since all interactions then occur in the atmosphere and are subject to large QCD backgrounds. We have not ex-

plored the analysis of atmospheric phenomena using surface arrays. For example, hadronic air showers initiated by proton- or neutrino-induced multi-W events may have features distinct from generic hadronic air showers. Among the exploitable features may be the longitudinal development of multi-W air showers (they should be shorter) or the transverse development (they should be wider due to the W-boson transverse momentum). Studies of these phenomena would require both large cross sections and a demonstration that the signal looks significantly different from the background. For example, one would have to be able to discern between multi-W showers and a hadronic shower initiated by heavy cosmic nuclei [42]. Since the studies of the composition of high-energy hadronic cosmic rays are still in their infancy, it is doubtful that multi-W phenomena would be immediately apparent in the context of air showers.

One of the advantages of underground detectors is that, unlike surface arrays which study atmospheric showers, they may be sensitive to very small point cross sections ($\simeq 1$ nb). For example, even for $\hat{\sigma}_0 = 100$ pb, $\sqrt{\hat{s}_0} = 4$ TeV, we would expect on the order of one muon bundle per year at large zenith angles in a DUMAND-size detector. Indeed, large-zenith-angle muons appear to promise a characteristic signature of neutrino-induced multi-W phenomena in cosmic rays.

VIII. CONCLUSIONS

We have demonstrated the plausibility of investigating multi-W phenomena in cosmic rays by searching for large-zenith-angle muon bundles in underground detectors. If the flux of high-energy neutrinos is as large as allowed by current Fly's Eye limits, then we have found background-free detection rates of a few neutrino-induced events per year in a DUMAND-size detector (if multi-W phenomena exist with point cross sections in the range of 1–100 nb and thresholds $\sqrt{\hat{s}_0} = 4$–20 TeV). However, our conclusions are subject to the caveat that a favorably large neutrino flux may, in reality, not be present. The construction of neutrino telescopes with large effective areas (~ 1 km^2) would make multi-W phenomena, if they exist at all, readily accessible in the realm of cosmic-ray physics.

ACKNOWLEDGMENTS

We gratefully acknowledge helpful conversations with S. Coutu, T. K. Gaisser, M. H. Salamon, P. Sokolsky, T. Stanev, and E. Zas. We especially thank R. D. Peccei for many clarifying discussions, a critical reading of the manuscript, and for bringing this problem to our attention. This work was supported by the Eloisatron Project (D.A.M.) and by the World Laboratory (R.R.).

*Electronic address: morris@uclahep.bitnet.
†Electronic address: rosenfeld@uclahep.bitnet.

[1] For reviews see A. Ringwald, lecture given at the International School of Subnuclear Physics, Erice, Italy, July 1990, Report No. CERN-TH-5949-90 (unpublished); R. D. Peccei, in *Baryon Number Violation at the SSC?*, Proceedings of the Santa Fe Workshop, Santa Fe, New Mexico, 1990, edited by M. Mattis and E. Mottola (World Scientific, Singapore, 1990).
[2] A. Ringwald, Nucl Phys. **B330**, 1 (1990); O. Espinosa, *ibid.* **B343**, 310 (1990).
[3] J. M. Cornwall, Phys. Lett. B **243**, 271 (1990); H. Goldberg, *ibid.* **246**, 445 (1990); M. B. Voloshin, Phys. Rev. D **43**, 1726 (1991); J. M. Cornwall and G. Tiktopoulos, Report No. UCLA-90-TEP-56 (unpublished).
[4] A. Ringwald and C. Wetterich, Nucl. Phys. **B353**, 303 (1991).
[5] G. 't Hooft, Phys. Rev. D **14**, 3432 (1976).
[6] V. V. Khoze and A. Ringwald, Nucl. Phys. **B355**, 351 (1991); M. Porrati, *ibid.* **B347**, 371 (1990).
[7] T. Banks, G. Farrar, M. Dine, D. Karabali, and B. Sakita, Nucl. Phys. **B347**, 581 (1990).
[8] G. R. Farrar and R. Meng, Phys. Rev. Lett. **65**, 3377 (1990).
[9] A. Ringwald, F. Schrempp, and C. Wetterich, DESY Report No. 90-127 (unpublished).
[10] A. Zichichi, in *ICOMAN '83*, Proceedings of the International Colloquium on Matter Nonconservation, Frascati, Italy, 1983, edited by E. Bellotti and S. Stipcich (INFN, Frascati, 1984); E. Bellotti, in *Proceedings of the Third ESO/CERN Symposium*, Bologna, Italy, 1988, edited by M. Caffo (Kluwer Academic, Boston, 1988).
[11] See, e.g., V. J. Stenger, in *Physics and Experimental Techniques of High Energy Neutrinos and VHE and UHE Gamma-Ray Particle Physics*, Proceedings of the Workshop, Little Rock, Arkansas, 1989, edited by G. B. Yodh, D. C. Wold, and W. R. Kropp [Nucl. Phys. B (Proc. Suppl.) **14A**, 153 (1990)].
[12] G. Domokos and S. Nussinov, Phys. Lett. B **187**, 372 (1987); J. Collins and F. Olness, *ibid.* **187**, 376 (1987); G. Domokos and S. Kovesi-Domokos, Phys. Rev. D **38**, 2833 (1988); G. Domokos, B. Elliot, S. Kovesi-Domokos, and S. Mrenna, Phys. Rev. Lett. **63**, 844 (1989).
[13] For a critical review, see J. M. Bonnet-Bidaud and G. Chardin, Phys. Rep. **170**, 325 (1988).
[14] E. Eichten, I. Hinchliffe, K. Lane, and C. Quigg, Rev. Mod. Phys. **56**, 579 (1984); **58**, 1065 (1986).
[15] L V. Gribov, E. M. Levin, and M. G. Ryskin, Phys. Rep. **100**, 1 (1983).
[16] C. Quigg, M. H. Reno, and T. P. Walker, Phys. Rev. Lett. **57**, 774 (1986).
[17] M. H. Reno and C. Quigg, Phys. Rev. D **37**, 657 (1988).
[18] See, for example, L. Durand and H. Pi, Phys. Rev. D **40**, 1436 (1989).
[19] M. F. Crouch *et al.*, Phys. Rev. D **18**, 2239 (1978); M. R. Krishnaswamy *et al.*, Pramana **19**, 525 (1982); R. Svoboda *et al.*, Astrophys. J. **315**, 420 (1987).
[20] Y. Oyama *et al.*, Phys. Rev. D **39**, 1481 (1989).
[21] T. K. Gaisser and T. Stanev, Nucl. Instrum. Methods **A235**, 183 (1985).
[22] C. Forti, H. Bilokon, B. Piazzoli, T. K. Gaisser, L. Satta, and T. Stanev, Phys. Rev. D **42**, 3668 (1990).
[23] T. K. Gaisser and T. Stanev, Phys. Rev. D **30**, 985 (1984).
[24] T. K. Gaisser and A. F. Grillo, Phys. Rev. D **36**, 2752

(1987).
[25] F. Halzen and E. Zas, in *Physics and Experimental Techniques of High Energy Neutrinos and VHE and UHE Gamma-Ray Particle Physics* [11], p. 60.
[26] L. B. Bezrukov and E. V. Bugaev, in *Proceedings of the DUMAND Summer Workshop,* Khabarovsk, USSR, 1979, edited by J. G. Learned (DUMAND Center, Honolulu, Hawaii, 1980), p. 227.
[27] A. N. Kalinovskii, N.V. Mokhov, and Yu. P. Nikitin, *Passage of High-Energy Particles Through Matter* (AIP, New York, 1989).
[28] T. Stanev (private communication).
[29] See, e.g., T. K. Gaisser, *Cosmic Rays and Particle Physics* (Cambridge University Press, Cambridge, England, 1990), for an introduction to the relevant techniques and references to the original literature.
[30] J. Kempa and J. Wdowczyk, J. Phys. G **9**, 1271 (1983).
[31] R. M. Baltrusaitis *et al.*, Phys. Rev. D **31**, 2192 (1985).
[32] J. H. MacGibbon and R. H. Brandenberger, Nucl. Phys. **B331**, 153 (1990).
[33] L. V. Volkova, Yad. Fiz. **31**, 1510 (1980) [Sov. J. Nucl. Phys. **31**, 784 (1980)].
[34] F. W. Stecker, Astrophys. J. **228**, 919 (1979).
[35] S. H. Margolis, D. N. Schramm, and R. Silberberg, Astrophys. J. **221**, 990 (1978).
[36] F. W. Stecker, C. Done, M. H. Salamon, and P. Sommers, Phys. Rev. Lett. **66**, 2697 (1991).
[37] K. Greisen, Phys. Rev. Lett. **16**, 748 (1966); G. T. Zatsepin and V. A. Kuzmin, Pis'ma Zh. Eksp. Teor. Fiz. **4**, 53 (1966) [JETP Lett. **4**, 78 (1966)].
[38] C. T. Hill and D. N. Schramm, Phys. Lett. **131B**, 247 (1983); Phys. Rev. D **31**, 564 (1985).
[39] P. Sokolsky, *Introduction to Ultrahigh Energy Cosmic Ray Physics* (Addison-Wesley, Reading, MA, 1989).
[40] F. Halzen, University of Wisconsin—Madison Report No. MAD/PH/663 (unpublished).
[41] T. K. Gaisser and T. Stanev, Phys. Rev. Lett. **54**, 2265 (1985); E. W. Kolb, M. S. Turner, and T. P. Walker, Phys. Rev. D **32**, 1145 (1985).
[42] P. Sokolsky (private communication).